IOP PUBLISHING JOURNAL OF PHYSICS D: APPLIED PHYSICS

J. Phys. D: Appl. Phys. **41** (2008) 085505 (4pp) doi:10.1088/0022-3727/41/8/085505

Electrification of a nanoporous electrode in a continuous flow

Yu Qiao[1], **Aijie Han and Venkata K Punyamurtula**

Department of Structural Engineering, University of California – San Diego, La Jolla, CA 92093-0085, USA

E-mail: yqiao@ucsd.edu

Received 10 December 2007, in final form 8 February 2008
Published 26 March 2008
Online at stacks.iop.org/JPhysD/41/085505

Abstract

By forcing an electrolyte solution to flow across a nanoporous electrode, a significant output voltage was measured. In contradiction to the classic streaming-potential theory, the output voltage was independent of the flow rate and the electrode distance. The discharge time was longer by orders of magnitude than the retention time. If the external resistance was relatively small, the voltage would eventually vanish. These unique phenomena can be attributed to the amplification effect of the large nanopore surface area on the mechanical disturbance of surface capacity.

1. Introduction

While liquid electrification at solid surfaces, such as stream-current generation of oil transported in a pipeline, is a well known phenomenon [1], its application in energy conversion has not received the necessary attention until recently when the processing techniques of nanoporous materials were relatively well developed [2–4]. Conventionally, nanoporous materials were used in the areas of chemical engineering and biomedical science for catalysis, absorption and adsorption, separation and purification, etc [5,6]. Conductive nanoporous materials include nanoporous carbons and carbon nanotubes, semiconductors, as well as metals and alloys [7]. They are often synthesized by templating techniques. By removing a continuous template phase through combustion or extraction, the empty space can be left in the network phase as nanopores [8, 9]. Other techniques, such as hydrothermal treatment and pressurized sintering, are also commonly utilized [10, 11].

As an electrolyte solution contacts a solid surface, a layered structure of solvated ions can be formed. The inner layer, which is often referred to as the Stern layer, is of the highest ion density and the lowest ion mobility; in the outer layer, which is known as the Gouy–Chapman layer, the ion structure is less ordered and the ion mobility is higher. As the liquid flows along the solid surface, a shear plane is formed, resulting in a zeta (ζ) potential [12]. The stream current caused by the net charges in the diffusive layer of a continuous flow in a circular channel can be assessed as $I = \pi d\sigma_0 v_0$ [13], where d is the channel size, σ_0 is the effective charge density and v_0 is the flow velocity. Consequently, a potential difference, ϕ^*, is developed:

$$\phi^* = 4\sigma_0 v_0 l_0/d \cdot \xi, \tag{1}$$

where l_0 is the channel length and ξ is the liquid conductivity. This electrokinetic phenomenon has been well appreciated in electropolishing, microflow control, biological research, etc [14], and has been studied intensively (e.g. [15–21]). Once the flow stops, the equilibrium in the inner and outer layers can be reestablished within a few microseconds [22]. Recently, stream currents were observed in silicon nanochannels [23,24]. However, the total electric energy would be rapidly consumed as the ion structure reached the steady state. One way to solve this problem is to increase the conductivity of the nanochannel surface, e.g. by using a nanoporous electrode. It is envisioned that as the liquid electrification takes place over the large nanopore surface, significant electric energy can be generated. Such a system can extract useful electricity from ambient mechanical motions, which are otherwise wasted or harmful.

2. Experimental

In the current study, a Chand–Eisenmann nanoporous monel was investigated. Monel is a stainless copper–nickel alloy [25]. The nanoporous structure was achieved by sintering pressurized monel nanoparticles. The nanopore diameter was around 460 nm. The as-received material was in cylinder form, with a diameter of 9.5 mm and a length of 19.1 mm.

[1] Author to whom any correspondence should be addressed.

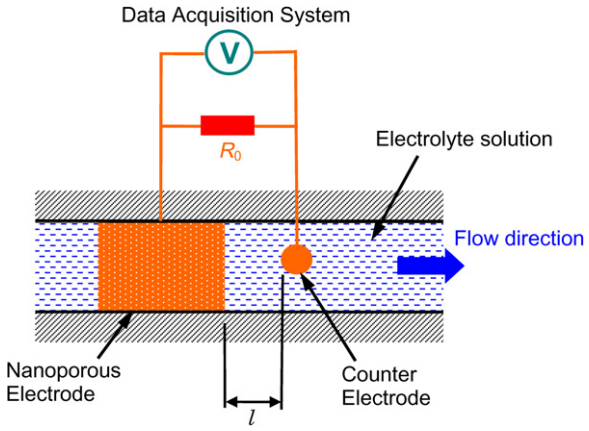

Figure 1. Schematic of the experimental setup.
(This figure is in colour only in the electronic version)

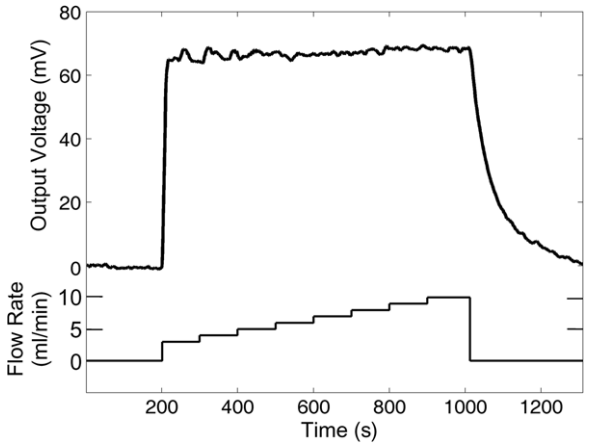

Figure 2. A typical measurement result of the output voltage. The external resistance is 1 MΩ.

The total pore surface area of each cylinder was 6.7 m^2. The mechanoelectric energy conversion system was formed by firmly clamping a nanoporous monel cylinder (the electrode) in a polyethylene pipe, as shown in figure 1. A counter electrode was placed 10–50 mm away from the monel cylinder. A continuous flow of 20 wt% aqueous solution of sodium chloride was forced through the electrode using a MasterFlex L/S 7518-10 digital drive. The monel cylinder and the counter electrode were connected by nichrome wires through a 1 MΩ resistor, R_0, across which the potential difference was measured by a National Instruments 6936E Data Acquisition (DA) board. The nanoporous monel cylinder was connected to the cathode of the DA board, and the counter electrode was connected to the anode.

Figure 2 shows a typical measurement result of the output voltage, ϕ, which, as will be discussed shortly, is different from ϕ^* in equation (1). Initially, the flow rate, Q, was zero. At time t_0, the digital drive was turned on and the flow rate was increased to the set point, and maintained at this level for 100 s. Then, the flow rate was increased gradually by 1 ml min^{-1} in each step. The step width was 100 s. Finally, the digital drive was shut down and the flow rate was abruptly decreased to zero. Similar measurements were performed for systems of different electrode distances, l, at various flow rates. The ϕ–Q and ϕ–l relationships are shown in figure 3.

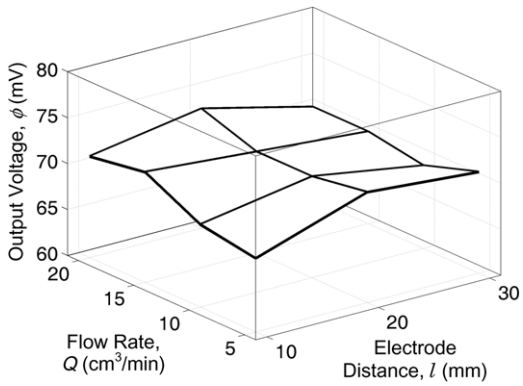

Figure 3. The output voltage as a function of the electrode distance and the flow rate.

3. Results and discussion

According to figure 2, as the electrolyte solution starts to flow, a significant output voltage is generated. After the pump is turned on, the value of ϕ rapidly rises from 0 to about 68 mV, and is stabilized at this level as the flow continues. As the flow rate changes, there is no detectable variation in output voltage. After the flow stops, it takes more than 300 s. for ϕ to decrease to 0. The measured voltage is positive, indicating that the potential of the electrode is higher than that of the counter electrode. Note that the output voltage is not caused by a redox reaction. If it were related to electrochemical reactions, it should be detectable when the flow stops or when the electrode is solid.

The observed phenomena are different from the predictions of the classic streaming-potential theory. First, the measured voltage is quite independent of the flow rate, which is more clearly shown in figure 3. As the flow rate increases, the variation in ϕ is small and random. This is contradictory to equation (1) that predicts a strong correlation between ϕ^* and v_0. Second, ϕ is insensitive to the electrode distance, l. As shown in equation (1), in an ordinary electrolyte flow, as the two electrodes are moved farther away from each other, the potential difference between them should increase linearly. Third, l is not an analogue to l_0. In a conventional electrokinetics setup, the potential difference is measured inside the flow channel. In the current study, because the pore surface is conductive, ϕ is measured between the electrode and the counter electrode outside the nanopores. Finally, as the flow stops, the decay of output voltage is slow, with the characteristic time close to that of diffusional transport. If the output voltage were directly caused by the ζ-potential, the discharge time should be comparable to the retention time. At room temperature, the retention time is usually at the microsecond level [26]. Furthermore, due to the relatively high electrolyte concentration, the Debye distance is around a few nanometres [27], which is quite small compared with the nanopore size, and thus the stream current should be dominated by the neutral bulk liquid phase. Note that these

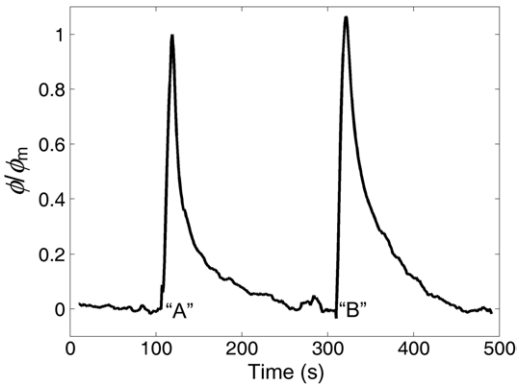

Figure 4. The output voltage as a function of time. The external resistance $R_0 = 100\,\Omega$ and the reference voltage $\phi_m = 19.6\,\text{mV}$.

observations are not dependent on the external resistance. As R_0 is changed in a broad range from 100 Ω to 1 MΩ, while the output potential can become time dependent, as will be discussed shortly, the above characteristics can always be observed. The measurement results of ϕ is also independent of the flow direction.

Figure 4 shows the output voltage as a function of time when the external resistance, R_0, was largely reduced to 100 Ω. In an ordinary stream-current system, if the resistance between the two electrodes is relatively small, a new equilibrium is established and the potential difference should be zero, since there is no return path. In the nanoporous system, however, a significant transient voltage is detected. At point A, the flow started and the voltage rapidly increased to the peak value of $\phi_m = 19.6\,\text{mV}$. As the flow continued, the voltage decreased gradually. At time B, the electrode and the counter electrode were disconnected, grounded for 5 min, and then reconnected. It can be seen that the energy conversion capacity was fully recovered. The flow rate was constant during the entire experiment. It is clear that, as the liquid flows, the equilibrium of ion structure at the solid–liquid interface is disrupted. The difference between figures 2 and 4 is caused by the change in resistance. The output potential difference can be stated as $\phi = \Delta\phi - \phi_0$, where $\Delta\phi$ is the difference between the potential differences across solid–liquid surfaces at the electrode and the counter electrode, and ϕ_0 is the potential difference in the liquid phase. Initially, when the liquid is at rest, both $\Delta\phi$ and ϕ_0 are zero, so is ϕ. When the liquid starts to flow, the ion distributions at the surfaces of the electrode and the counter electrode become different, which can be attributed to the confinement effect of pore walls as well as the difference in effective flow rate in nanopores and in the bulk liquid phase [28–30]. Consequently, $\Delta\phi$ is developed. When R_0 is large, the current between the electrode and the counter electrode is negligible, and the difference in charge density can be maintained constant. In the liquid phase, ϕ_0 is actually dominated by the stream-current effect along the polyethylene pipe, which is negligible, primarily because the Debye length is much smaller than the pipe diameter. Hence, the output voltage is associated with the surface polarization effect, independent of the electrode distance and having a long characteristic discharge time.

When R_0 is relatively small, the excess surface charges would move from the low-potential end to the high-potential one, forming a transient current. The total charge associated with the current is around 15 mC, and the electric energy is about 0.2 mJ. Since the total surface area of the nanoporous electrode is $6.7\,\text{m}^2$, the density of the excess counter charges (electrons) is $2.2\,\text{mC m}^{-2}$, or $1.4 \times 10^{16}\,e\,\text{m}^{-2}$. In the 20 wt% sodium chloride solution, the average cation density is $2.04 \times 10^{27}\,e\,\text{m}^{-3}$, and in a surface layer a few nanometres thick the cation density is 10^{19}–$10^{20}\,e\,\text{m}^{-2}$. That is, as the liquid flows, the variation in surface ion density is around 0.01–0.1%. This change is insensitive to the flow rate, probably because that for the thin interface layer even the lowest flow rate, which is about $700\,\mu\text{m s}^{-1}$, is still large and thus the disturbance effect has been saturated. Once the transient current vanishes, the energy conversion capacity of the system is lost. However, as shown in figure 4, during the grounding process, the system configuration rapidly returns to its initial state and the accumulated excess charges could form the transient current again, indicating that the transient current is directly related to the motion of counter charges (electrons) in the solid phase, rather than the ion motion in the liquid phase.

4. Concluding remarks

Clearly, the above discussion provides only a qualitative framework for understanding the experimental data. More detailed study needs to be carried out to analyse the effects of electrolyte concentration, pH value, etc. Nevertheless, it has been validated that semi-continuous mechanoelectric energy conversion can be achieved by maintaining a flow across a nanoporous electrode. Contradictory to the classic electrokinetic theory, the potential difference is insensitive to the flow rate and the electrode distance, and the discharging process is quite slow. If the external resistance is relatively small, the output voltage would vanish as the new equilibrium is established.

Acknowledgments

The materials preparation was supported by The Army Research Office under Grant No W911NF-05-1-0288. The analysis was supported by The National Science Foundation under Grant No CMS-0623973. Special thanks are also due to Dr Kake Zhu for the useful discussions.

References

[1] Moore A D 1968 *Electrostatics* (New York: Laplacian Press)
[2] Yang J, Lu F Z, Kostiuk L W and Kwok D Y 2003 *J. Micromech. Microeng.* **13** 963
[3] van der Heyden F H J, Stein D and Dekker C 2005 *Phys. Rev. Lett.* **95** 116104
[4] Qiao Y, Punyamurtula V K and Han A 2007 *J. Power Sources* **164** 931
[5] Zukal A 2007 *Chem. Listy* **101** 208
[6] Dubbeldam D, Snurr R Q 2007 *Mol. Simul.* **33** 305
[7] Polarz S and Smarsly B 2002 *J. Nanosci. Nanotechnol.* **2** 581
[8] Cejka J and Zilkova N 2000 *Chem. Listy* **94** 278

[9] Ciesla U and Schuth F 1999 *Microporous Mesoporous Mater.* **27** 131
[10] Lee J, Kim J and Hyeon T 2006 *Int. J. Nanotechnol.* **3** 253
[11] Grosso D, Boissiere C, Nicole L and Sanchez C 2006 *J. Sol–Gel Sci. Technol.* **40** 141
[12] Crowley J M 1999 *Fundamentals of Applied Electrostatics* (New York: Laplacian Press)
[13] Bard A J and Faulkner L R 2000 *Electrochemical Methods: Fundamentals and Applications* (New York: Wiley)
[14] Prosser A J and Franses E I 2001 *Colloids Surf.* A **178** 1
[15] Fu X, Li B M, Zhang J F, Tian F Z and Kwok D Y 2007 *Int. J. Mod. Phys.* C **18** 693
[16] Sheffer M R, Reppert P M and Howie J A 2007 *Rev. Sci. Instrum.* **78** 094502
[17] Xuan X C and Sinton D 2007 *Microfluid Nanofluid* **3** 723
[18] Sherwood J D 2007 *Phys. Fluids* **19** 053101
[19] Sides P J, Newman J, Hoggard J D and Prieve D C 2006 *Langmuir* **22** 9765
[20] Renaud L, Kleimann P and Morin P 2004 *Electrophoresis* **25** 123
[21] Darnet M and Marquis G J 2004 *Hydrology* **285** 114
[22] Taylor D M and Secker P E 2003 *Industrial Electrostatics* (Hertfordshire, UK: Research Studies Press)
[23] Yang J, Lu F Z, Kostiuk L W and Kwok D Y 2005 *J. Nanosci. Nanotechnol.* **5** 648
[24] van der Heyden F H J, Stein D, Besteman K, Lemay S G and Dekker C 2006 *Phys. Rev. Lett.* **96** 224502
[25] Sinha A 2002 *Physical Metallurgy Handbook* (New York: McGraw-Hill)
[26] Metzler R and Klafter J 2000 *Phys. Rep.* **339** 1
[27] Bockris J O, Reddy A K N and Gamboa-Aldeco M 1998 *Modern Electrochemistry* (Dordrecht: Kluwer)
[28] Qiao Y, Cao G and Chen X 2007 *J. Am. Chem. Soc.* **129** 2355
[29] Han A and Qiao Y 2006 *J. Am. Chem. Soc.* **128** 10348
[30] Han A and Qiao Y 2007 *Langmuir* **23** 11396